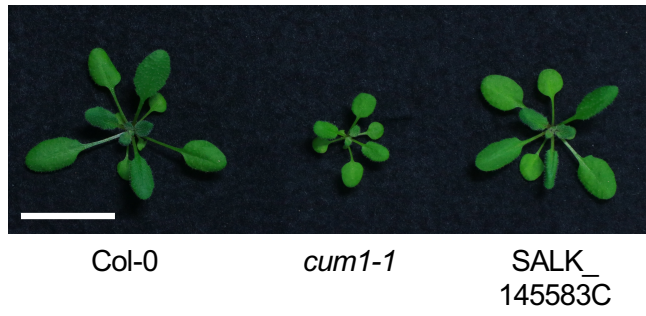


(a)



(b)

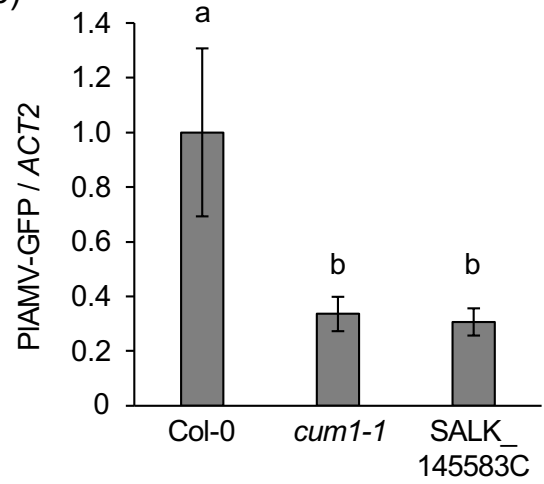


Fig. S1. Loss of eIF4E1 inhibits PIAMV infection. (a) Representative photos of 4-week-old Col-0 and two eIF4E1-deficient *A. thaliana* mutant lines (*cum1-1* and SALK_145583C). The scale bar indicates 2 cm. (b) Col-0 and two *eif4e1* mutant lines (*cum1-1* and SALK_145583C) were mechanically inoculated with PIAMV-GFP. Viral RNA levels in the inoculated leaves at 4 dpi were quantified by qRT-PCR. The data are presented as the mean \pm SE obtained from two independent repeat experiments. The mean in Col-0 was set as the standard (1.0). Statistically significant differences are indicated by different letters (Steel-Dwass test, $p < 0.05$).

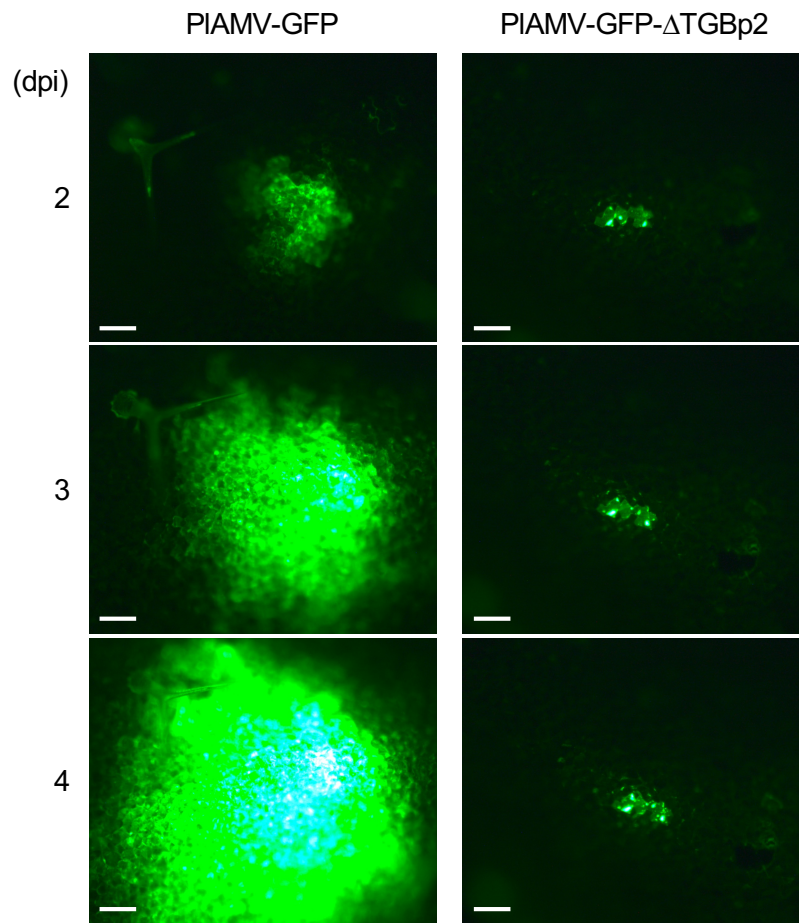


Fig. S2. Time course observation of fluorescent foci of infection. Col-0 plants were mechanically inoculated with PIAMV-GFP or PIAMV-GFP- Δ TGBp2 and the development of fluorescent foci of infection was followed by fluorescence microscopy at 2–4 dpi. Representative images are shown. The scale bars indicate 100 μ m.

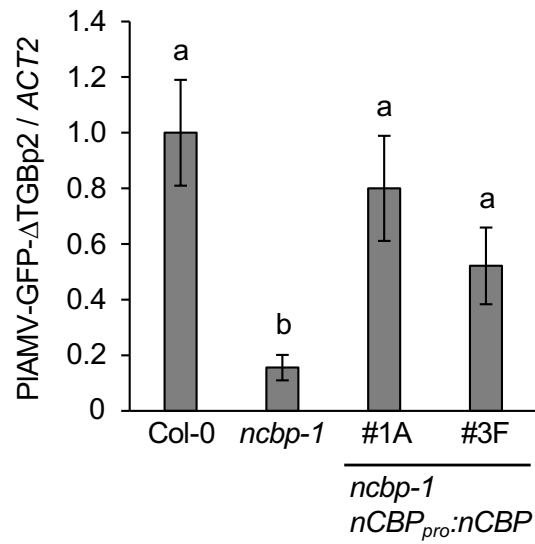


Fig. S3. Functional validation of nCBP in cellular accumulation of PIAMV by transgenic complementation. Col-0, *ncbp-1*, and nCBP-complemented lines #1A and #3F (17) were mechanically inoculated with PIAMV-GFP-ΔTGBp2. Viral RNA levels in the inoculated leaves at 4 dpi were quantified by qRT-PCR. The data are presented as the mean \pm SE obtained from two independent repeat experiments. The mean in Col-0 was set as the standard (1.0). Statistically significant differences are indicated by different letters (Steel-Dwass test, $p < 0.05$).